

# Quantitative Analysis of Corneal Energy Dissipation and Corneal and Orbital Deformation in Response to an Air-Pulse in Healthy Eyes

Hans R. Vellara,<sup>1</sup> Noor Q. Ali,<sup>1</sup> Akilesh Gokul,<sup>1</sup> Jason Turuwhenua,<sup>2</sup> Dipika V. Patel,<sup>1</sup> and Charles N. J. McGhee<sup>1</sup>

<sup>1</sup>Department of Ophthalmology, New Zealand National Eye Centre, University of Auckland, Auckland, New Zealand

<sup>2</sup>School of Optometry and Visual Sciences, University of Auckland, Auckland, New Zealand

Correspondence: Dipika V. Patel, Department of Ophthalmology, Private Bag 92019, University of Auckland, Auckland, New Zealand; dipika.patel@auckland.ac.nz.

Submitted: June 1, 2015

Accepted: September 8, 2015

Citation: Vellara HR, Ali NQ, Gokul A, Turuwhenua J, Patel DV, McGhee CNJ. Quantitative analysis of corneal energy dissipation and corneal and orbital deformation in response to an air-pulse in healthy eyes. *Invest Ophthalmol Vis Sci.* 2015;56:6941-6947. DOI:10.1167/iovs.15-17396

**PURPOSE.** To examine and evaluate ocular biomechanical metrics and additionally derived corneal and orbital components using a noncontact Scheimpflug-based tonometer (CorVis ST) in a population of healthy eyes.

**METHODS.** A total of 152 eyes of 152 participants were examined by slit-lamp biomicroscopy, corneal tomography, and the CorVis ST (CST). This determined the distribution of outputs from the CST, such as deformation amplitude (DA), and additionally derived parameters, including maximum corneal deformation (MCD), maximum orbital deformation (MOD), and corneal energy dissipation (CED).

**RESULTS.** The mean age of participants was  $35.88 \pm 13.8$  years. Deformation amplitude significantly correlated with age ( $r = 0.24$ ,  $P = 0.002$ ) but not sex or ethnicity ( $P > 0.05$ ). Multiple linear regression analysis revealed significant correlations between DA and age ( $r = 0.19$ ,  $P = 0.006$ ) and DA and IOP ( $r = -0.59$ ,  $P < 0.001$ ). Age correlated with MCD ( $r = 0.20$ ,  $P = 0.01$ ), MOD ( $r = 0.18$ ,  $P = 0.03$ ), and CED ( $r = 0.39$ ,  $P < 0.001$ ). Males had a lower MOD than females (0.24 vs. 0.26 mm, respectively,  $P = 0.01$ ); however, there were no differences in MCD or CED between sexes ( $P > 0.05$ ). There were no significant differences between ethnicities for MCD, MOD, and CED ( $P > 0.05$ ). Multiple linear regression analysis revealed significant correlations between MCD and IOP ( $r = -0.65$ ,  $P < 0.001$ ), CED and age ( $r = 0.41$ ,  $P < 0.001$ ), CED and IOP ( $r = 0.28$ ,  $P = 0.001$ ), and between CED and central corneal thickness (CCT) ( $r = -0.36$ ,  $P < 0.001$ ).

**CONCLUSIONS.** The isolation of the corneal component (MCD) should be used when analyzing deformation characteristics in diseases that only affect the cornea. This study establishes a baseline for a population of healthy eyes. Future publications will identify differences in MCD, MOD, and CED between healthy and diseased populations.

**Keywords:** cornea biomechanics, maximum corneal deformation, corneal energy dissipation, maximum orbital deformation, CorVis ST

The cornea is a viscoelastic structure that exhibits classic biomechanical properties such as elasticity, creep, stress relaxation, and hysteresis.<sup>1</sup> These mechanical properties stem from the constituent components of the cornea and therefore are governed by factors such as the extracellular matrix and the organization of collagen fibers.<sup>2</sup>

The assessment of corneal biomechanical properties has a number of potential clinical applications such as improving the accuracy of IOP measurements,<sup>3,4</sup> the diagnosis of keratoconus (KC),<sup>5</sup> assessing the biomechanical effects of corneal collagen crosslinking (CXL),<sup>6</sup> and assessing the risk of post-LASIK ectasia.<sup>7,8</sup>

Recently, the CorVis ST (CST; Oculus, Wetzlar, Germany) was introduced as a clinical tool for the assessment of corneal biomechanical properties in vivo. The CST is a noncontact tonometer that emits a collimated air-pulse (3.05-mm diameter) that is coupled with a high-speed Scheimpflug camera (4330 frames/sec, aligned at 45 degrees to the cornea). The air-pulse causes the cornea to deform inward into a concave configura-

tion before returning to its initial shape. The real-time video analysis of the deformation profile allows for a number of unique measurements to be made, including deformation amplitude (DA).<sup>9</sup> This is the total displacement of the corneal apex from its initial position to the point of highest concavity. Previously, studies have described DA as a solely corneal reaction.<sup>10-12</sup> However, the in vivo response to an air-pulse is not purely corneal.<sup>13</sup> It includes an indirect and collateral globe displacement secondary to the transfer of energy to the orbital tissue and extraocular muscles.<sup>13</sup> Unfortunately, the inbuilt CST software (v6.07r24) does not provide the isolated pure corneal and orbital components. However, separated components may be derived through external analysis of the CST videos.<sup>14</sup>

Application of a cyclic load to viscoelastic materials results in a loss of energy per cycle due to the inherent viscosity in the system.<sup>15</sup> By calculating the area within the loading and unloading curves of the stress-strain graph, the dissipated energy can be determined quantitatively.<sup>16</sup> Ishii et al.<sup>17</sup> previously described the area within the graph produced as

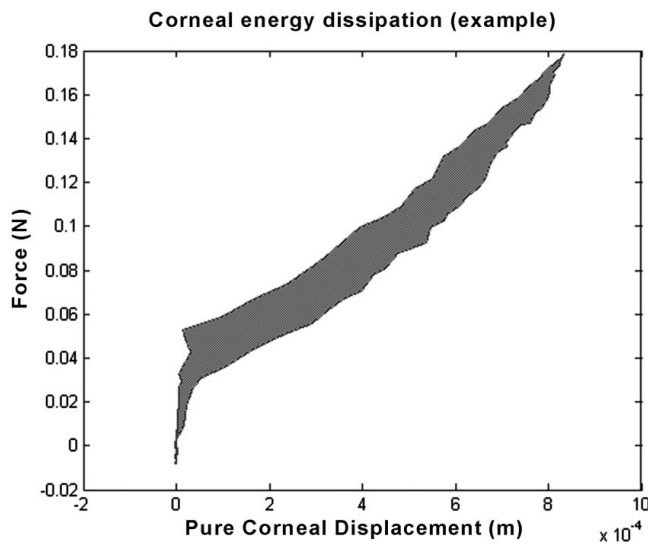


FIGURE 1. An example of an output graph for CED.

“elastic hysteresis.” They utilized a noncontact tonometer in conjunction with a high-speed camera angled at 90° to the cornea and plotted the change in corneal apex position (strain) against the amount of force applied onto the cornea by the air-pulse (stress). However, the camera could not image the cornea past the applanation point.<sup>17</sup>

This problem is overcome by using the videos provided by the CST, in which the corneal apex position during the whole deformation process can be tracked (including past the applanation point). This is then refined to exclude the orbital deformation, and correlated to the force applied by the air-pulse. We have termed the area within the resulting graph produced as corneal energy dissipation (CED).

The aim of this study included the determination of the distribution of CST parameters, separated components (corneal and orbital), and CED in a population of healthy eyes. It also describes the repeatability of the separated components and hence establishes baseline data. Finally, the statistically significant and nonsignificant correlations for age, IOP, maximum keratometry ( $K_{MAX}$ ), and central corneal thickness (CCT) with the additional parameters were examined. This is to aid in attempting to control for parameters that are potential confounders when comparing between healthy and diseased populations.

**METHODS**

**Participants**

All participants were recruited from staff, relatives of staff, and relatives of patients at the Greenlane Clinical Centre, Auckland District Health Board, New Zealand. Exclusion criteria were previous ocular trauma/surgery or infections, contact lens wear, or any systemic or ocular disease that may affect the cornea.

TABLE 1. The Mean, SD, and Range of Values for Each Parameter Measured by the CorVis ST in Healthy Eyes ( $n = 152$ )

Parameters	Mean	SD	Range
IOP, mm Hg	13.7	2.2	8.0 to 21.5
CCT, $\mu\text{m}$	544	34	460 to 633
DA, mm	1.07	0.10	0.82 to 1.32
Peak distance (PD), mm	4.21	1.33	2.06 to 7.04
Radius of curvature (RoC), mm	7.41	0.82	5.37 to 9.55
First applanation length (A1L), mm	1.81	0.26	0.93 to 2.72
Velocity inward ( $V_{IN}$ ), m/s	0.16	0.02	0.1 to 0.24
Second applanation length (A2L), mm	1.84	0.41	1.03 to 2.83
Velocity outward ( $V_{OUT}$ ), m/s	-0.35	0.06	-0.66 to -0.19
Time to highest concavity ( $T_{HC}$ ), ms	17.01	0.49	15.29 to 18.32
Time to first applanation ( $T_1$ ), ms	7.19	0.24	6.59 to 8.2
Time to second applanation ( $T_2$ ), ms	22.24	0.62	20.79 to 23.64

For each participant, demographic data, such as age, sex, and ethnicity, were collected. Only the right eye was examined for each participant unless it fell under one of the exclusion criteria listed above, in which case, the left eye was examined.

Informed consent was obtained from all participants and the study design adhered to the tenets of the Declaration of Helsinki. The study protocol was approved by the University of Auckland human ethics committee (reference number 010853).

**Examinations**

The examinations were performed by experienced investigators (HRV, NQA, and AG). All participants were examined by slit-lamp biomicroscopy to confirm a healthy ocular status and to ensure that none of the exclusion criteria were met.

Corneal tomography was examined using the Pentacam HR (Oculus, Wetzlar, Germany).

Corneal biomechanical properties were assessed using the CST. Once the participants’ cornea was centered using the alignment markers provided on the machine’s display, the instrument automatically emitted the collimated air-pulse. The force of the air-pulse at the nozzle is 60 mm Hg. The device captures a two-dimensional image sequence using a Scheimpflug camera system. This sequence spanned a measurement time of less than 32 ms, over which time the cornea went through first inward applanation (flattening), deformation to maximum concavity, and, finally, the second outward applanation as the cornea returned to its original shape. Individual frames within the video are analyzed by the inbuilt CST software to produce various unique parameters.<sup>9</sup>

**Corneal and Orbital Deformation Algorithm**

The CST videos or the files with an extension of .CST, were imported into a script file in Matlab (version 8.4.0.150421 [R2014b]; Natick, MA, USA). The individual images in the video

TABLE 2. Repeatability of MCD, MOD, and CED for Three Measurements Taken 2 to 5 Minutes Apart

Parameter	Precision	Repeatability	CV, %	Intraclass Correlation (95% Confidence Interval)	P
MCD	0.09 mm	0.13 mm	5.08	0.88 (0.74–0.95)	<0.001
MOD	0.05 mm	0.08 mm	8.74	0.88 (0.75–0.95)	<0.001
CED	$3.55 \times 10^{-6}$ Nm	$5.01 \times 10^{-6}$ Nm	13.0		

TABLE 3. Repeatability of MCD, MOD, and CED Measured at Four Different Times of the Day

Parameter	Precision	Repeatability	CV, %	Intraclass Correlation (95% Confidence Interval)	P
MCD	0.09 mm	0.13 mm	5.21	0.76 (0.60-0.88)	<0.001
MOD	0.05 mm	0.07 mm	7.80	0.71 (0.53-0.85)	<0.001
CED	$4.21 \times 10^{-6}$ Nm	$5.95 \times 10^{-6}$ Nm	16.2		

are processed using methods previously described extensively by Koprowski et al.<sup>14,18</sup> Image analysis includes detection of the anterior corneal edge using the Canny method, morphologic image processing (close operation), and corneal contour.<sup>18</sup> The resulting data are then used to derive pure corneal ( $L_{TR}(n, i)$ ) and orbital ( $L_{TO}(n, i)$ ) components from the total displacement ( $L_T(n, i)$ ) (where  $n$  indexes pixels in individual columns  $n \in (1, N)$ , and  $i$  indexes individual frames in the video  $i \in (1, D)$ , respectively).<sup>14,18</sup> Derivation of separated components is owed to the visible corneal contour at the edge of the video and has been explained elsewhere.<sup>14,18</sup>

The method has been validated by comparing the results from their algorithms to data from the CST.<sup>14</sup> The correlated data revealed an error of less than 1% in mean SD. From the resulting analysis we obtained the maximum change in pure corneal displacement over the course of the video. We have termed this as the maximum corneal deformation (MCD). Following the notation of Koprowski, this is

$$MCD = \max_n \left( \max_i \left( L_{TR}(n, i) \right) \right). \quad (1)$$

The change in pure orbital displacement was calculated at the same location on the cornea and termed as the maximum orbital deformation (MOD). Denoting the location of the MCD by indices ( $n_{MCD}, i_{MCD}$ ) we obtain

$$MOD = \max_i \left( L_{TO}(n_{MCD}, i) \right). \quad (2)$$

### Corneal Energy Dissipation

A cyclic corneal deformation pattern results from the CST air-pulse. Perfectly elastic materials undergo identical loading and unloading phases; however, viscoelastic materials like the cornea have a portion of the energy lost or dissipated. This is due to the inherently viscous proteoglycan matrix.

Analysis of CED was performed by making amendments to the script file in Matlab as follows. The corneal apex was monitored over the course of the video. This is then refined to exclude the influence of orbital deformation ( $L_{TR}(n_{max}, i)$ ), as previously described by Koprowski.<sup>14</sup> Data regarding the force emitted was exported from the CST (mm Hg). Given the air-pulse has a diameter of 3.05 mm, the force can be converted to newtons. The change in pure corneal displacement at the corneal apex is then plotted against the air-pulse force emitted, producing characteristic loading and unloading curves. The area between these curves quantifies CED (Nm). A typical example of CED from a healthy eye has been provided in Figure 1.

TABLE 4. Repeatability of the MCD, MOD, and CED for Measurements Taken at the Same Time of the Day, on Different Days

Parameter	Precision	Repeatability	CV, %	Intraclass Correlation (95% Confidence Interval)	P
MCD	0.12 mm	0.17 mm	6.63	0.66 (0.42-0.83)	<0.001
MOD	0.06 mm	0.08 mm	9.40	0.49 (0.19-0.75)	<0.001
CED	$4.51 \times 10^{-6}$ Nm	$6.38 \times 10^{-6}$ Nm	16.4		

### Statistical Analyses

Statistical analysis was performed using SPSS software version 22.0 (IBM Corporation, Chicago, IL, USA) and Prism software version 6.01 (GraphPad, La Jolla, CA, USA). The normality of the data was tested using the D'Agostino and Pearson omnibus normality test.

Descriptive statistical analysis was performed on baseline characteristics. A Wilcoxon matched-pairs signed rank test was used for differences between DA, MCD, and MOD. Two-tailed Spearman's correlation coefficient was used to measure statistical dependence between nonparametric variables. Significant differences between sexes were investigated using the Mann-Whitney *U* test. A Kruskal-Wallis test was conducted to explore the differences in variables between ethnicities. Newly derived parameters (MCD, MOD, and CED) were tested for repeatability using the Bland-Altman methodology. The mean within-subject SD ( $S_w$ ) was determined. Precision (Pr) and repeatability were calculated using the formulas  $1.96 \times S_w$  and  $2.77 \times S_w$ , respectively. The mean of within-subject means was divided by  $S_w$  to derive the coefficient of variation (CV). Intraclass correlation (ICC) was calculated by using ANOVA. An ICC of more than 0.70 and a CV less than 20% were considered highly repeatable; an ICC of more than 0.60 and CV less than 20% were considered fairly repeatable.

Multiple linear regression analysis was performed to determine if age, IOP, CCT, and  $K_{MAX}$  are significant predictors of DA, MCD, MOD, or CED. Only highly repeatable and reliable CST parameters have been included in the multiple linear regression analysis.<sup>5,19</sup> Central corneal thickness and  $K_{MAX}$  were obtained using the Pentacam HR (v6.07r29).

*P* values of 0.05 or less were considered to be statistically significant.

## RESULTS

### Characteristics of Healthy Corneas

A total of 152 healthy subjects were recruited with a mean age of  $35.88 \pm 13.8$  years (range, 13-74 years). There was a larger proportion of females (62%,  $n = 95$ ) than males (38%,  $n = 57$ ). Most participants were of European ethnicity (53.8%,  $n = 81$ ), followed by Indian subcontinent (18.6%,  $n = 29$ ), Southeast Asian (11.5%,  $n = 18$ ), Pacific Island Nations (5.1%,  $n = 8$ ), Middle Eastern (4.5%,  $n = 7$ ), Maori (4.5%,  $n = 6$ ), and African descent (1.9%,  $n = 3$ ).

Values for all CST parameters are presented in Table 1.

The mean DA was  $1.07 \pm 0.10$  mm. There was a significant correlation between DA and age ( $r = 0.24$ ,  $P = 0.002$ ; Fig. 2); however, there were no significant differences in DA between sexes ( $P = 0.63$ ) or ethnicities ( $P = 0.20$ ). Multiple linear

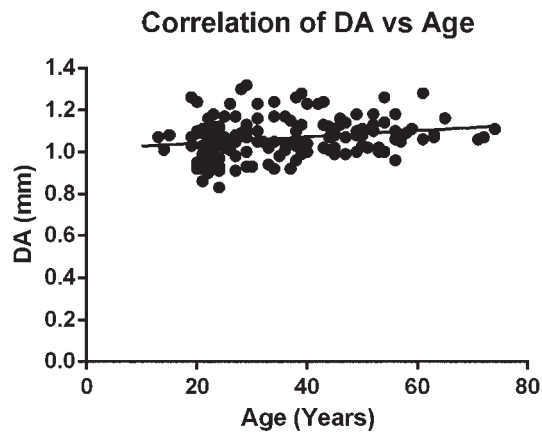


FIGURE 2. Correlation between DA and age in healthy eyes ( $n = 152$ ).

regression analysis revealed that DA was significantly positively correlated with age ( $r = 0.19$ ,  $P = 0.006$ ) and negatively correlated to IOP ( $r = -0.59$ ,  $P < 0.001$ ).

### Repeatability

In a subgroup of 23 healthy eyes, three examinations taken 2 to 5 minutes apart on the same day demonstrated high repeatability in MCD and MOD. For the examinations performed at four different times of day, MOD and MCD were highly repeatable. For examinations taken at the same time of day on three different days, MCD was fairly repeatable. ICC analysis for CED measurements was not possible, as several score values of zero made for minimal variance (an error message that reads “scale or part of scale has zero variance and will be bypassed” was displayed on SPSS). However, the CV was below 20% in all instances (2–5 minutes apart, four different times of the day, and three examinations performed on three different days).

The precision, repeatability, CV, and ICC are summarized for three measurements taken 2 to 5 minutes apart (Table 2), three measurements taken at different times of day (Table 3), and three measurements taken on three different days (Table 4).

### Maximum Corneal Deformation and Maximum Orbital Deformation in Healthy Corneas

The mean MCD and MOD were  $0.80 \pm 0.09$  mm and  $0.25 \pm 0.05$  mm, respectively (Table 5). There was a significant correlation between MCD and age ( $r = 0.20$ ,  $P = 0.01$ ; Fig. 3A), MOD and age ( $r = 0.18$ ,  $P = 0.03$ ; Fig. 3B), and MOD and  $K_{MAX}$  ( $r = 0.17$ ,  $P = 0.04$ ; Fig. 3C). Although there were no significant differences among ethnicities for both parameters ( $P > 0.05$ ), there was a significantly higher MOD in males compared with females ( $0.24$  vs.  $0.26$  mm, respectively,  $P = 0.01$ ) but no differences between sexes for MCD ( $P = 0.30$ ).

Multiple linear regression analysis revealed a significant correlation between MCD and IOP ( $r = -0.65$ ,  $P < 0.001$ ); however, MOD did not correlate significantly with the parameters included in the multiple linear regression.

Wilcoxon matched-pairs signed rank test revealed statistically significant differences ( $P < 0.001$ ) among all three groups of values tested (DA, MCD, and MOD).

### Corneal Energy Dissipation in Healthy Corneas

The mean CED was  $(2.02 \pm 0.65) \times 10^{-5}$  Nm (Table 5). There was a significant correlation between CED and age ( $r = 0.39$ ,  $P < 0.001$ ; Fig. 4) and no significant differences in CED between

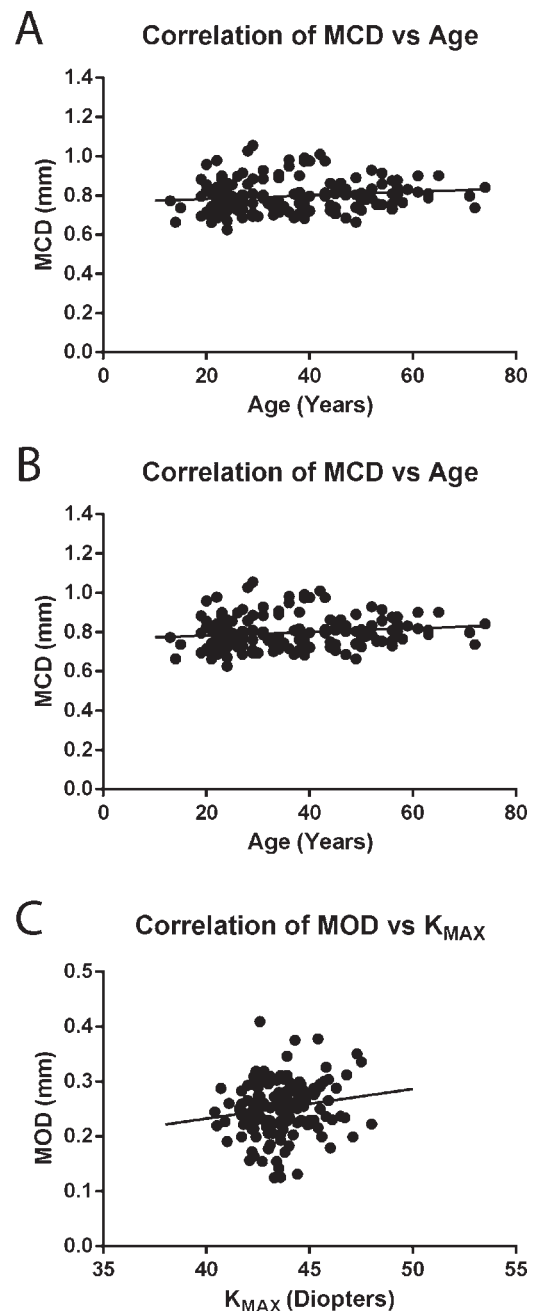


FIGURE 3. Correlation between (A) MCD and age, (B) MOD and age, (C) MOD and  $K_{MAX}$  in healthy eyes ( $n = 152$ ).

sexes ( $P = 0.87$ ) or ethnicities ( $P = 0.94$ ). Multiple linear regression analysis revealed significant correlations between CED and age ( $r = 0.41$ ,  $P < 0.001$ ), CED and IOP ( $r = 0.28$ ,  $P = 0.001$ ), and between CED and CCT ( $r = -0.36$ ,  $P < 0.001$ ).

### DISCUSSION

The in vivo eyeball reaction to an air-pulse includes contributions from the cornea, orbital tissue, and extraocular muscles.<sup>13</sup> Koprowski<sup>14</sup> described methods of analyzing CST videos to derive supplementary parameters accounting for these components. These additional methods of analyzing CST videos have not been investigated in healthy corneas. We

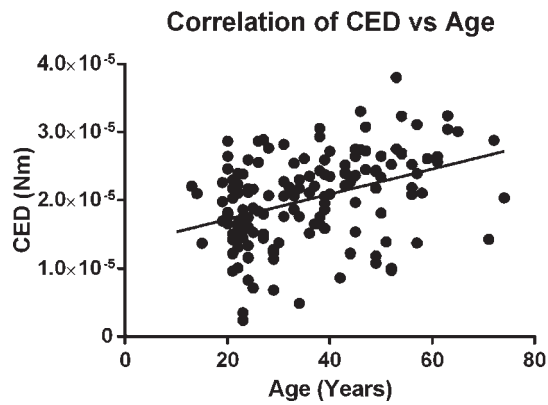


FIGURE 4. Correlation between CED and age for healthy eyes ( $n = 152$ ).

determined the distribution of CST parameters, and separated components and the correlation of these parameters with age, sex, ethnicity, corneal thickness, and corneal curvature in a population with healthy corneas.

Previous studies have considered DA as an exclusively corneal phenomenon<sup>10-12</sup>; however, this study provides evidence of the distribution and significant difference between DA (provided by the device) and the isolated corneal (MCD) and orbital (MOD) components in a population of healthy corneas. Isolation of the orbital component should be used when analyzing deformation characteristics in diseases that only affect the cornea. Furthermore, future publications need to consider these additional parameters, as they could identify whether the corneal or the orbital component contributes to the differences in overall DA.

The aging cornea is known to change its stromal microstructure. The cornea undergoes natural glycation-induced crosslinks causing an increased cross-sectional area within collagen fibers and fibrillar molecules.<sup>20,21</sup> Corresponding biomechanical increases in corneal tissue stiffness have been observed through ex vivo inflation testing.<sup>22-24</sup> However, biomechanical changes with age using in vivo testing methods are still debated.

There are two commercially available devices that claim to measure biomechanical properties of the cornea in vivo, the Ocular Response Analyzer (ORA; Reichert, Inc., Depew, NY, USA) and the CST, although direct comparisons between these instruments are not possible, as the pressure profiles of the ORA vary between measurements, whereas the CST has a consistent pressure profile in all measurements.<sup>25</sup> Any comparisons made between these machines must adjust for these differences before drawing conclusions.

Several studies have investigated the relationship between ORA parameters and age.<sup>8,26-29</sup> Foster et al.<sup>26</sup> demonstrated a significant correlation with age for both output parameters

(corneal hysteresis [CH] and corneal resistance factor [CRF]) in a large study involving 4184 eyes; however, several factors were not incorporated into a multivariate analysis, including IOP, CCT, and keratometry. Other studies have reported similar observations but with weaker correlations.<sup>8,27,28</sup> Conversely, Kirwan, et al.<sup>29</sup> showed no correlation between CH and age in a subset of children.

In the current study, there was a significant correlation between age and DA, and the correlation remained after isolating the corneal component. This is in agreement with Leung et al.,<sup>11</sup> who demonstrated a statistically significant, weak relationship ( $r = 0.002$ ) between age and DA in a group of normal, glaucoma, and glaucoma-suspect eyes. Tian et al.<sup>12</sup> also described a significant positive correlation ( $r = 0.43$ ) between age and DA. Conversely, others have discovered no significant correlations between age and DA.<sup>5,30</sup>

An increase in DA with age is counterintuitive to ex vivo studies that exhibit increased stiffness with age<sup>22-24</sup>; however, the deformation response to an air-pulse has been claimed to be largely influenced by corneal interlamellar sliding resistance.<sup>31</sup> These resistance forces would be influenced by the content and distribution of the proteoglycan matrix interspersed between collagen fibrils and collagen lamellae. Age is associated with an increase in cross-sectional collagen fibril and fibrillar molecular area but with decreased interfibrillar spacing.<sup>20,21,32</sup> This indicates reduced proteoglycan substance in the aged cornea, which may subsequently cause decreased interlamellar sliding resistance. Furthermore, the nonenzymatic crosslinks shown to occur with age may not affect these resistance forces.<sup>20</sup>

Loss or atrophy of orbital fat is a natural aging process.<sup>33</sup> Observations in this study imply a more compliant orbit with age, as MOD increased with age ( $r = 0.18$ ,  $P = 0.03$ ). This is in agreement with a previous study by Frueh,<sup>34</sup> which demonstrated that the force required to displace the orbit posteriorly a fixed distance using a contact lens was lower in the older age group ( $>45$ ) when compared with the younger age group ( $>45$ ). Furthermore, our data revealed a statistically significant ( $P = 0.01$ ) difference in MOD between sexes. The magnitude of this difference (0.02 mm) is not clinically significant.

Hysteresis is a crucial parameter for understanding corneal biomechanical behavior. The physical property describes the difference between the loading and unloading curves.<sup>16</sup> The behavior hails from the viscous component dissipating energy within the viscoelastic system.<sup>25</sup> Analysis of corneal hysteresis could reveal the viscous damping effect in the complex viscoelastic cornea.<sup>24</sup> The area between the loading and unloading curves for a deformation response to an air-pulse has been previously described by Ishii et al.<sup>17</sup> as "elastic hysteresis." However, the cornea was not imaged past the appplanation point in the deformation process and the orbital response to the air-pulse was not isolated.<sup>17</sup>

In the current study, CED incorporates the corneal apex position past the appplanation point and considers only the

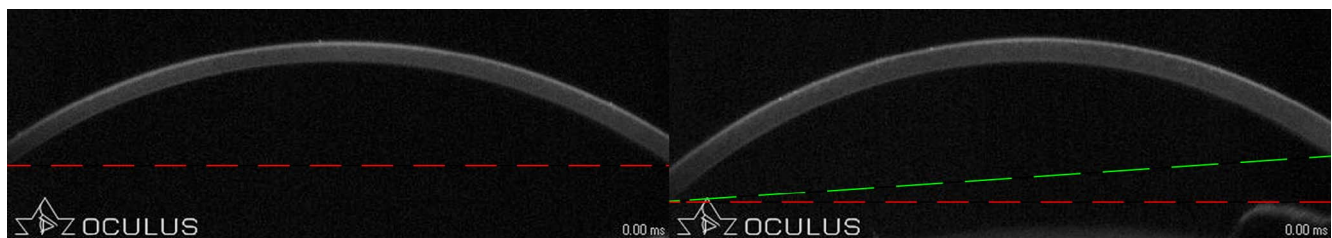


FIGURE 5. Comparison of two normal CST videos showing differences in corneal rotation between measurements. Red lines are perfectly horizontal in both images. The green line joins the posterior cornea at the edges of the image. The difference between the red and green lines demonstrates the amount of rotation in the video.

**TABLE 5.** The Mean  $\pm$  SD and Range of Values for DA, MCD, MOD, and CED in Healthy Corneas ( $n = 152$ )

	Mean $\pm$ SD	Range
DA, mm	1.07 $\pm$ 0.10	0.83–1.32
MCD, mm	0.80 $\pm$ 0.09	0.63–1.06
MOD, mm	0.25 $\pm$ 0.05	0.13–0.41
CED, Nm	(2.02 $\pm$ 0.65) $\times 10^{-5}$	(0.24–3.80) $\times 10^{-5}$

pure corneal response. A significant correlation between age and CED was observed in this dataset. However, ex vivo inflation studies were not able to demonstrate statistically significant differences in hysteresis with age.<sup>24</sup> In this study, the positive correlation identified between age and CED is in contrast to the observations of Ishii et al.,<sup>17</sup> who reported a statistically significant decrease in hysteresis with age.

Hysteresis is not only dependent on the viscosity of the material but the nature of the pressure applied onto the cornea. Previously published in vivo and ex vivo studies used different instruments that use alternate pressure characteristics. Thus, direct comparisons in hysteresis values between these studies are not possible.

A potential limitation of this study is that the true corneal apex position may have been displaced slightly during the deformation process or, alternatively, the air-pulse profile may not have been directly applied at the center of the cornea.

As shown in Figure 5, normal measurements can be taken where the apex is tilted away from the center of the air-pulse profile. This could impact the deformation analysis.<sup>6</sup> The true apex cannot be followed unless a method of tracking the apex is provided or the air-pulse is applied correctly in every measurement. Lago et al.<sup>35</sup> proposed a methodology for an in vivo estimation of the biomechanical behavior. The biggest contributor to dissimilarity between simulated deformed corneas and real deformed corneas were in cases in which the positions of the air-pulse were not aimed directly at the center.<sup>35</sup> Thus, misaligned measurements can cause significant changes to deformation characteristics.

Additional research is needed to predict the magnitude of change in deformation characteristics corresponding to variations in tilt. This would first require the development of a reliable and repeatable method of deriving the amount of tilt in individual videos.

A three-dimensional imaging technique would allow a thorough understanding of the energy dissipated in a viscoelastic structure; however, the CST provides two-dimensional images. Additionally, CED only incorporates information over a single dimension. This reduction in complexity may have contributed to the results observed in this study.

Future studies will develop methods of accounting for this tilt and analyze the impact of these additional components between normal and diseased populations.

### Acknowledgments

Disclosure: **H.R. Vellara**, None; **N.Q. Ali**, None; **A. Gokul**, None; **J. Turuwheua**, None; **D.V. Patel**, None; **C.N.J. McGhee**, None

### References

1. Elsheikh A, Wang D, Pye D. Determination of the modulus of elasticity of the human cornea. *J Refract Surg.* 2007;23:808–818.
2. Lombardo M, Lombardo G, Carbone G, et al. Biomechanics of the anterior human corneal tissue investigated with atomic force microscopy. *Invest Ophthalmol Vis Sci.* 2012;53:1050–1057.

3. Burgoyne CF, Crawford Downs J, Bellezza AJ, et al. The optic nerve head as a biomechanical structure: a new paradigm for understanding the role of IOP-related stress and strain in the pathophysiology of glaucomatous optic nerve head damage. *Prog Retin Eye Res.* 2005;24:39–73.
4. Smedowski A, Weglarz B, Tarnawska D, et al. Comparison of three intraocular pressure measurement methods including biomechanical properties of the cornea. *Invest Ophthalmol Vis Sci.* 2014;55:666–673.
5. Ali NQ, Patel DV, McGhee CN. Biomechanical responses of healthy and keratoconic corneas measured using a noncontact Scheimpflug-based tonometer. *Invest Ophthalmol Vis Sci.* 2014;55:3651–3659.
6. Steinberg J, Katz T, Mousli A, et al. Corneal biomechanical changes after crosslinking for progressive keratoconus with the corneal visualization Scheimpflug technology. *J Ophthalmol.* 2014;2014:579190.
7. Dupps WJ Jr, Wilson SE. Biomechanics and wound healing in the cornea. *Exp Eye Res.* 2006;83:709–720.
8. Ortiz D, Piñero D, Shabayek MH, et al. Corneal biomechanical properties in normal, post-laser in situ keratomileusis, and keratoconic eyes. *J Cataract Refract Surg.* 2007;33:1371–1375.
9. Ambrósio R Jr, Ramos I, Luz A, et al. Dynamic ultra high speed Scheimpflug imaging for assessing corneal biomechanical properties. *Rev Bras Ophthalmol.* 2013;72:99–102.
10. Hon Y, Lam AK. Corneal deformation measurement using Scheimpflug noncontact tonometry. *Optom Vis Sci.* 2013;90:e1–e8.
11. Leung CK, Ye C, Weinreb RN. An ultra-high-speed Scheimpflug camera for evaluation of corneal deformation response and its impact on IOP measurement. *Invest Ophthalmol Vis Sci.* 2013;54:2885–2892.
12. Tian L, Wang D, Wu Y, et al. Corneal biomechanical characteristics measured by the CorVis Scheimpflug technology in eyes with primary open-angle glaucoma and normal eyes [published online ahead of print February 1, 2015]. *Acta Ophthalmol.* doi:10.1111/aos.12672.
13. Kling S, Marcos S. Contributing factors to corneal deformation in air puff measurements. *Invest Ophthalmol Vis Sci.* 2013;54:5078–5085.
14. Koprowski R, Lyssek-Boron A, Nowinska A, et al. Selected parameters of the corneal deformation in the corvis tonometer. *Biomed Eng Online.* 2014;13:55.
15. Lapshin RV. Analytical model for the approximation of hysteresis loop and its application to the scanning tunneling microscope. *Rev Sci Instrum.* 1995;66:4718–4730.
16. Hopkinson B, Williams GT. The elastic hysteresis of steel. *Proc R Soc Lond A.* 1912;87:502–511.
17. Ishii K, Saito K, Kameda T, Oshika T. Elastic hysteresis in human eyes is an age-dependent value. *Clin Experiment Ophthalmol.* 2013;41:6–11.
18. Koprowski R. Automatic method of analysis and measurement of additional parameters of corneal deformation in the corvis tonometer. *Biomed Eng Online.* 2014;13:150.
19. Chen X, Stojanovic A, Hua Y, et al. Reliability of corneal dynamic Scheimpflug analyser measurements in virgin and post-PRK eyes. *PLoS One.* 2014;9:e109577.
20. Malik NS, Moss SJ, Ahmed N, et al. Ageing of the human corneal stroma: structural and biochemical changes. *Biochim Biophys Acta.* 1992;1138:222–228.
21. Daxer A, Misof K, Grabner B, et al. Collagen fibrils in the human corneal stroma: structure and aging. *Invest Ophthalmol Vis Sci.* 1998;39:644–648.
22. Elsheikh A, Wang D, Brown M, et al. Assessment of corneal biomechanical properties and their variation with age. *Curr Eye Res.* 2007;32:11–19.

23. Elsheikh A, Geraghty B, Rama P, et al. Characterization of age-related variation in corneal biomechanical properties. *J R Soc Interface*. 2010;7:1475-1485.
24. Elsheikh A, Wang D, Rama P, et al. Experimental assessment of human corneal hysteresis. *Curr Eye Res*. 2008;33:205-213.
25. Vellara HR, Patel DV. Biomechanical properties of the keratoconic cornea: a review. *Clin Exp Optom*. 2015;98:31-38.
26. Foster PJ, Broadway DC, Garway-Heath DF, et al. Intraocular pressure and corneal biomechanics in an adult British population: the EPIC-Norfolk eye study. *Invest Ophthalmol Vis Sci*. 2011;52:8179-8185.
27. Kamiya K, Shimizu K, Ohmoto F. Effect of aging on corneal biomechanical parameters using the ocular response analyzer. *J Refract Surg*. 2009;25:888-893.
28. Fontes BM, Ambrosio R Jr, Alonso RS, et al. Corneal biomechanical metrics in eyes with refraction of -19.00 to +9.00 D in healthy Brazilian patients. *J Refract Surg*. 2008;24:941-945.
29. Kirwan C, O'Keefe M, Lanigan B. Corneal hysteresis and intraocular pressure measurement in children using the reichert ocular response analyzer. *Am J Ophthalmol*. 2006;142:990-992.
30. Valbon BF, Fontes BM, Alves MR. Effects of age on corneal deformation by non-contact tonometry integrated with an ultra-high-speed (UHS) Scheimpflug camera. *Arq Bras Oftalmol*. 2013;76:229-232.
31. Wollensak G, Sporn E, Mazzotta C, et al. Interlamellar cohesion after corneal crosslinking using riboflavin and ultraviolet A light. *Br J Ophthalmol*. 2011;95:876-880.
32. Kanai A, Kaufman HE. Electron microscopic studies of corneal stroma: aging changes of collagen fibers. *Ann Ophthalmol*. 1973;5:285-287 passim.
33. Yip CC, Gonzalez-Candial M, Jain A, et al. Lagophthalmos in enophthalmic eyes. *Br J Ophthalmol*. 2005;89:676-678.
34. Frueh BR. Graves' eye disease: orbital compliance and other physical measurements. *Trans Am Ophthalmol Soc*. 1984;82:492-598.
35. Lago M, R perez M, Mart nez-Mart nez F, et al. A new methodology for the in-vivo estimation of the elastic constants that characterize the patient-specific biomechanical behavior of the human cornea. *J Biomech*. 2014;48:38-43.